Journal of Solid State Chemistry 210 (2014) 242–250

Contents lists available at ScienceDirect

Journal of Solid State Chemistry

journal homepage: www.elsevier.com/locate/jssc

Controlled release of ibuprofen by meso–macroporous silica

E. Santamaría *, A. Maestro, M. Porras, J.M. Gutiérrez, C. González

Department of Chemical Engineering, Faculty of Chemistry, University of Barcelona, Barcelona, Martí i Franqués 1-11, Catalonia 08028, Spain

ARTICLE INFO

Article history:
Received 17 August 2013
Received in revised form
11 November 2013
Accepted 22 November 2013
Available online 5 December 2013

Keywords:
Meso–macroporous material
Silica
Ibuprofen controlled release

ABSTRACT

Structured meso–macroporous silica was successfully synthesized from an O/W emulsion using decane as a dispersed phase. Sodium silicate solution, which acts as a silica source and a poly(ethylene oxide)–poly(propylene oxide)–poly(ethylene oxide) ($EO_{19}PO_{39}EO_{19}$) denoted as P84 was used in order to stabilize the emulsion and as a mesopore template. The materials obtained were characterized through transmission electron microscopy (TEM), scanning electron microscopy (SEM), small-angle X-ray diffraction scattering (SAXS) and nitrogen adsorption–desorption isotherms. Ibuprofen (IBU) was selected as the model drug and loaded into ordered meso–macroporous materials. The effect of the materials' properties on IBU drug loading and release was studied. The results showed that the loading of IBU increases as the macropore presence in the material is increased. The IBU adsorption process followed the Langmuir adsorption isotherm. A two-step release process, consisting of an initial fast release and then a slower release was observed. Macropores enhanced the adsorption capacity of the material; this was probably due to the fact that they allowed the drug to access internal pores. When only mesopores were present, ibuprofen was probably adsorbed on the mesopores close to the surface. Moreover, the more macropore present in the material, the slower the release behaviour observed, as the ibuprofen adsorbed in the internal pores had to diffuse along the macropore channels up to the surface of the material. The material obtained from a highly concentrated emulsion was functionalized with amino groups using two methods, the post-grafting mechanism and the co-condensation mechanism. Both routes improve IBU adsorption in the material and show good behaviour as a controlled drug delivery system.

1. Introduction

Ordered mesoporous materials refer to materials with pore diameters in the 2–50 nm range possessing long-range order [1]. These materials possess unique structural characteristics and offer a wide range of potential applications. While searching for new high-surface area and ultra-large pore catalytic materials, scientist at Mobil Copr discovered that some of their synthetic procedures yielded solid, powdery products characterized by the presence of regular, ordered pores with diameters from 1.5 to over 10 nm and a high surface area [2,3]. Different structures can be obtained by carefully choosing the template, normally a surfactant. Surfactants act as structure-directing agents, so a surfactant chain-length variation may result in an increase or decrease of the mesopore sizes obtained.

Since the discovery of ordered mesoporous materials, many surfactants have been studied as potential structure-directing agents. The surfactant aggregates are used as templates to develop mesoporous materials with a variety of textures and structures [4]. These porous materials have attracted attention because of the wide variety of applications they are suitable for, and are particularly useful for the preparation of catalysts, drug delivery systems, sensors and chromatographic materials [5–7].

The incorporation of macropores in mesoporous materials combines the benefits of the mesoporous and the macroporous structures [8]. The addition of macropores can improve the efficiency of mesoporous materials as they enhance mass transport and reduce diffusion limitations [9–11]. In these materials, the macropores act as channels and facilitate the transport of molecules that have to be adsorbed in the mesopores. It has been demonstrated that hierarchical materials containing both interconnected macroporous and mesoporous structures have enhanced properties compared to materials with uniform pores. This is due to the increased mass transport through the material and maintenance of a specific surface area on the level of mesopore systems [12].

Various authors [13,14] have cited a very popular method for preparing macroporous materials, i.e. the emulsion-templating approach. Emulsions are defined as dispersions of a liquid (dispersed phase) inside another immiscible liquid (continuous phase). In order to obtain meso–macroporous materials, the continuous phase of the emulsion must be formulated in such a

* Corresponding author. Tel.: +34 679972602.
E-mail addresses: esthersantamaria@ub.edu, esther.santamaria@gmail.com (E. Santamaría).

0022-4596/$ - see front matter © 2013 Elsevier Inc. All rights reserved.
http://dx.doi.org/10.1016/j.jssc.2013.11.031

way that the mesostructure is formed, while the drops of emulsion will produce the macropores. Emulsions are classified as direct emulsions or oil in water (O/W), where the continuous phase is the aqueous one and oil is the dispersed phase, and inverse emulsions (W/O), where the oil is the continuous phase and the aqueous phase is the dispersed one.

In the present work, meso–macroporous materials were prepared via emulsion templating from an inorganic precursor, sodium silicate, already successfully used by other authors for the preparation of mesoporous materials [15]. The most commonly used sources of silica were TEOS and TMOS, instead of a sodium silicate solution. Sodium silicate presents advantages: neither ethanol nor methanol, which could destroy the mesopore structure, is freed, and they are cheaper than TEOS or TMOS.

Due the stable structure of mesoporous silica and its well-defined properties, these materials are ideal as a support for drug and protein encapsulation. In recent years, several researchers have described the use of mesoporous materials as drug delivery systems [16–25]. Controlled drug delivery systems can achieve precise spatial and temporal delivery of therapeutics agents to the target site. Generally, controlled drug delivery systems maintain drug concentrations within the optimum range in the precise sites of the body, which improves the therapeutic efficacy and reduces toxicity [26]. While smaller drug molecules and biomolecules can be accommodated in mesoporous materials with both smaller and bigger pore sizes, larger drug molecules require materials with bigger pore diameters [27]. Mesoporous silica materials contain residual silanol groups that can further be functionalized further by different organic groups in order to modify their surface properties [28,29]. This creates favourable surface-drug interactions, which in turn results in the materials' improved adsorption affinity for drug molecules. Lin and co-workers have shown that the organic functionalization of mesoporous materials also influences their biocompatibility [30]. In addition to surface functional groups, the morphology and size of the mesoporous materials also have an important influence on drug release characteristics [31].

Generally, surface functionalization of mesoporous silica materials via covalent bonding of organic groups can be achieved by two methods. i.e. post-grafting synthesis [29] and co-condensation [29]. Although the post-grafting method results in well-ordered, functionalized, mesostructured materials, it often produces non-uniformly distributed organic groups because the organic moieties may congregate more on the channel pore mouth and the exterior surfaces [32]. The co-condensation synthetic method of producing mesoporous materials involves a one-step procedure and allows better control of the loading and distribution of organic groups [33], although it often produces materials with less well-ordered mesoporous structures. The most frequently studied drug to be adsorbed is ibuprofen, since it is one of the most commonly used anti-inflammatory drugs and a model for this drugs type due to its relatively small size (1 nm).

2. Materials and methods

2.1. Materials

The triblock copolymer of poly(ethylene oxide)-*b*-poly(propylene oxide)-*b*-poly(ethylene oxide) Pluronic P84, $(EO)_{19}(PO)_{39}(EO)_{19}$ was supplied by Sigma Aldrich. Sodium silicate solution (Na_2O ~10.6% and SiO_2 ~26.5%) was used as a silica source and was supplied by Sigma Aldrich. Ethanol (96%), HCl (37%), and potassium cloride and sodium hydroxide were purchased from Panreac. Ibuprofen (> 98%) was purchased from TCI Chemicals Europe. Hexane (95%) and (3-aminopropyl) triethoxysilane (APTES) (> 98%) were supplied by Sigma Aldrich. Dialysis bags Cellu-Sep T3/Nominal MWCO: 12,000–14,000 were provided by Vertex Technics. Deionized water was used in all samples.

2.2. Methods

2.2.1. Ordered meso–macroporous silica material preparation

Ordered meso–macroporous silica materials were prepared using the emulsion template process. First, water and surfactant were mixed and kept under stirring at 50 °C to ease the melting of the surfactant. Later, the dispersed phase, decane, was added drop by drop until the desired dispersed phase fraction was reached. Once the emulsion was formed, the sodium silicate solution was added along with the concentrated HCl to trigger the hydrolysis reaction of the silicate [15]. The resulting mixture was stirred for 0.5 h and placed in an oven at 100 °C for 24 h to let the silicate polymerize in the aqueous phase of the emulsion, the external phase, thus producing a network of ordered mesopores.

The solid product was filtered off and dried at room temperature. The product was then dispersed in ethanol:HCl (1 M) 1:1 mixture (50 g), filtered off, dried and calcined at 550 °C for 5 h in order to eliminate the residual surfactant. The final appearance of the material was a white coloured powder.

2.2.2. Material functionalization

2.2.2.1. Post-grafting functionalization process. About 0.9 g of the material was mixed with 12 mL of APTES and 30 mL of toluene [34]. The mixture was gently stirred for 24 h and 50 °C in a closed bottle in order to prevent evaporation. The resulting material was filtered off and dried at room temperature.

2.2.2.2. Co-condensation functionalization. The material was synthesized as described in Section 2.2.1 and 12 mL of APTES was added [35] at the same time as the sodium silicate solution. The resulting mixture was stirred for 0.5 h and placed in an oven at 100 °C for 24 h in order to let the silicate polymerize in the aqueous phase of the emulsion. The solid product was washed and filtered off several times in order to eliminate the surfactant used.

2.2.3. Ibuprofen adsorption process

Typically, 50 mg of the material was put in 5 mL of hexane containing different concentrations of ibuprofen (IBU) (5, 10, 15, 20 and 35 mg/mL) in a closed bottle to prevent evaporation of the hexane and under gentle magnetic stirring for 72 h. The concentration of ibuprofen in hexane was determined through an UV spectrophotometer at 280 nm by collecting 3 mL of hexane filtered using a syringe filter.

2.2.4. Ibuprofen release experiments

The mesoporous material (100 mg) was placed into 10 mL of IBU solution in hexane (35 mg/mL) and stirred at room temperature for 72 h in a closed bottle to prevent evaporation of the hexane. The loaded materials were then filtered and dried at room temperature for 24 h. A 50 mg of the resulting materials was put into a dialysis bag and immersed in 50 mL of simulated body fluid (SBF, pH 7.4) [36-37] at 37 °C under magnetic stirring at 100 rpm.

2.2.5. Characterization

2.2.5.1. Transmission electron microscopy (TEM). The porous material were examined using a TEM (JEOL JEM-2100 microscope with an acceleration voltage of 200 kV). In order to prepare the sample for TEM analysis, the material was dispersed in ethanol by sonication for 5 min. The dispersion was dropped onto a copper grid coated with carbon film and dried at room temperature.

Chart 1
Relation of the carried out experiments: specific surface area (S_{BET}), pore diameter (ϕ) and pore volume (V_p) as a function of the oil fraction (weight). Water, surfactant, HCl and sodium silicate quantities are indicated.

Experiment	Water (g)	*P*84 (g)	Sodium silicate (g)	HCl (g)	Decane (g)	Dispersed phase	S_{BET} (m^2/g)	ϕ (nm)	V_p (cm^3/g)
P84_meso	20	1	3	6	0	0.00	600 ± 30	4.01 ± 0.10	0.65 ± 0.10
P84_20%	20	1	3	6	7.5	0.20	412 ± 20	4.14 ± 0.20	0.63 ± 0.15
P84_50%	20	1	3	6	30	0.50	330 ± 15	4.19 ± 0.15	0.51 ± 0.12
P84_75%	20	1	3	6	90	0.75	154 ± 10	8.47 ± 1.20	0.30 ± 0.05

2.2.5.2. Scanning electron microscopy (SEM). In this study, SEM (HITACHI S-4100 with carbon coated operated at 15 keV) was used to observe the morphology of the samples.

2.2.5.3. SAXS measurements. Small-angle X-ray diffraction scattering (SAXS) measurements were used to determine the structure of the mesoporous materials. Measurements were performed in a Hecus X-ray Systems GMBH Graz, equipped with a Siemens Kristalloflex 760 (K-760) generator. The temperature of the samples was fixed using a Peltier Anton Paar (25–300 °C) controller. The radiation wavelength was 1.54 nm.

2.2.5.4. N_2-sorption analysis. The specific surface area, mean pore diameter and pore volume of the meso–macroporous silica materials were determined by N_2-sorption analysis using a Micromeritics Tristar 300 instrument at −196 °C. Prior to each measurement, the samples were degassed at 120 °C for 6 h. The specific surface areas were estimated using the BET method. The pore diameter and pore size distribution were determined using the BJH method from the adsorption branch of the isotherm.

2.2.5.5. FT-IR. Powdered materials were pressed into a tungsten mesh grid and installed in an in situ FTIR transmission cell. Measurements were performed using a Thermo Scientific Nicolet iZ10, ATR diamond and detector DTGS with a spectral resolution of 4 cm^{-1} and a spectral range of 4000 to 525 cm^{-1}.

3. Results

3.1. Material characterization

A series of experiments was carried out (Chart 1) in order to study the influence of the dispersed phase on the porous material properties.

SAXS was used to determine the type of structure of the material obtained. In Fig. 1, the SAXS patterns for all of the samples with different contents in the dispersed phase are shown. In the first one, no oil fraction was used and, as can be observed, it is the sample with the most defined peaks. There are three peaks indexed as [1 0 0], [1 1 0], and [2 0 0], which can be associated with a well-ordered, two-dimensional (2D) hexagonal mesostructure, in accordance with the original reports [38–41]. This structure is the most common for triblock copolymers such as P84 that usually produce SBA-15 material. For the material with a dispersed phase fraction of 0.20, three peaks are detected in the SAXS pattern. The three reflections are not as well defined as the material without oil and seem located at q ratios $1:\sqrt{3}:2$, showing a possible hexagonal symmetry. The unit cell dimension ($a_0 = 2d_{100}/\sqrt{3}$), which corresponds to the sum of the pore diameter and the thickness of the pore wall, was calculated in accordance with Bragg's law and its value was 9.19 nm.

For a dispersed phase fraction of 0.50 the first peak found corresponds to an 11.8 nm cell dimension. The intensity of the peaks obtained is low due to the fact that the materials possess a large quantity of macropores. This result confirms the data

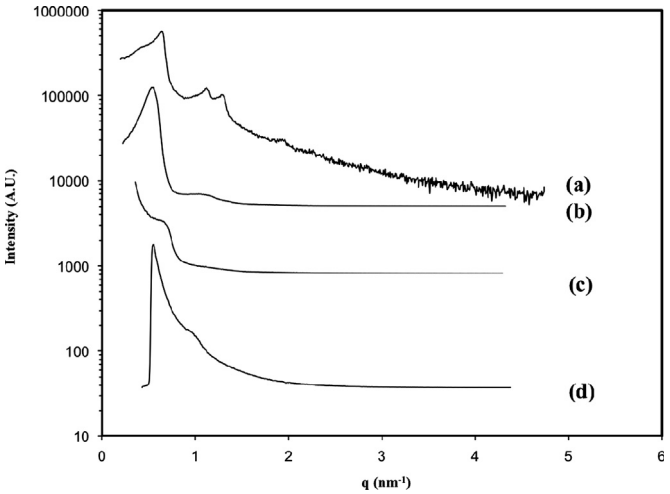

Fig. 1. SAXS pattern of obtained material with (a) no oil fraction (b) 0.20 oil fraction (c) 0.50 oil fraction and (d) 0.75 oil fraction.

reported by Du et al. [42] and Blin et al. [43], which would indicate that the higher the dispersed phase fraction used, the bigger the cell dimension of the material obtained.

Fig. 2 shows several representative scanning electron micrographs (SEM) of the synthesized silica. It shows how the macropore density increases as the dispersed phase fraction is increased. When more macropores exist, the effective thickness of the material is lower and, therefore, the SAXS peaks present less intensity. These materials present porosity at the nanometric and micrometric scale.

The sample with a dispersed phase of 0.75 (Fig. 2d) results in the typical image of macroporous material, in which the macropores occupy a large part of the material's volume and are separated by a thin layer of material. The macropores have the shape of the droplets in highly concentrated emulsions.

However it is unclear whether the hexagonal symmetry that is observed through SAXS, is linked to the organization of the wall of mesoporous material that surrounds the macropores, or is simply due to the macropore structure itself.

The TEM images (Fig. 3) show how the meso–macroporous materials are clearly ordered in their mesostructure, with well-oriented channels. Fig. 3a and b shows the characteristic honeycomb arrangement. From these observations, it can be concluded that the walls surrounding the macropores have a structured network of mesopores.

Fig. 3c and d show that some polyhedra corresponding to the macropores of the material (more than 50 nm) can be observed surrounded by thin walls of meso-sized pores. The bigger macropores were observed through SEM (Fig. 2).

Nitrogen adsorption–desorption isotherms and the corresponding BJH pore size distributions are shown in Fig. 4. This shows how they vary depending on the dispersed phase fraction used. According to the BDDT classification [44], isotherm type IV, which is typical of mesoporous materials, is obtained, but at high

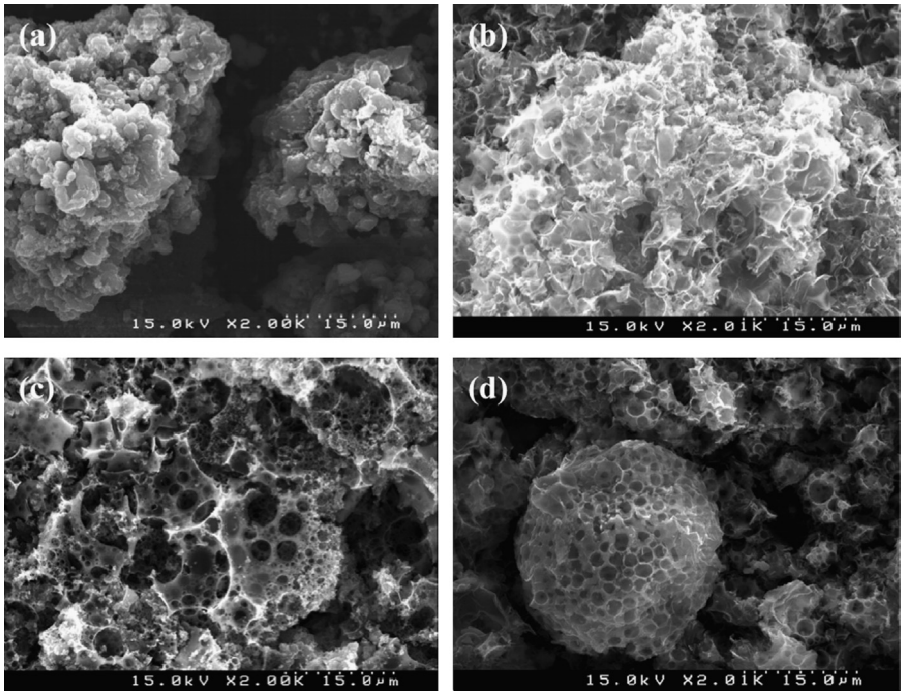

Fig. 2. SEM images from different materials obtained for different fraction of oil. (a) P84_meso (b) P84_20% (c) P84_50% and (d) P84_75%.

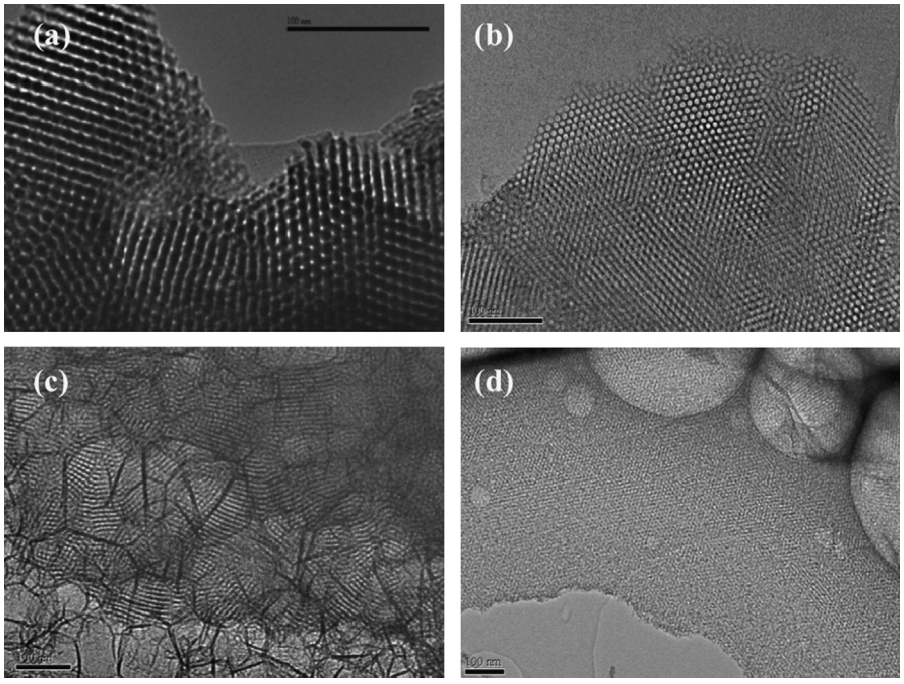

Fig. 3. TEM images of different materials obtained for different fraction of oil. (a) P84_meso (b) P84_20% (c) P84_50% and (d) P84_75%.

relative pressures the isotherms present a rise that is typical of macroporous materials. The higher the dispersed phase fraction used, the larger the indicative zone of macroporosity in the isotherm, due to the presence of more drops of the emulsion, which generated macropores, increase the density of macropores in the material. These conclusions are similar to those obtained by Stébé et al. [45], although in that case, the mesopores did not present any order for a dispersed phase fraction above to 0.45.

Pore size distributions show a sharp peak corresponding to a pore diameter of around 4 nm but for the material obtained with a dispersed phase fraction of 0.75, the distribution is wider than the other materials. This is due to the high presence of macropores. Emulsion droplets can range in size from microns to nanometers.

Fig. 4 also shows nitrogen adsorption–desorption isotherms corresponding to the materials after ibuprofen adsorption. In all cases, the hysteresis loop decreased and the specific surface reduced, which would indicate the successful adsorption of the ibuprofen. Pore size distributions were modified because ibuprofen was sometimes adsorbed in the entrance of the mesochannel, leading to a reduction in the size of the remaining pores.

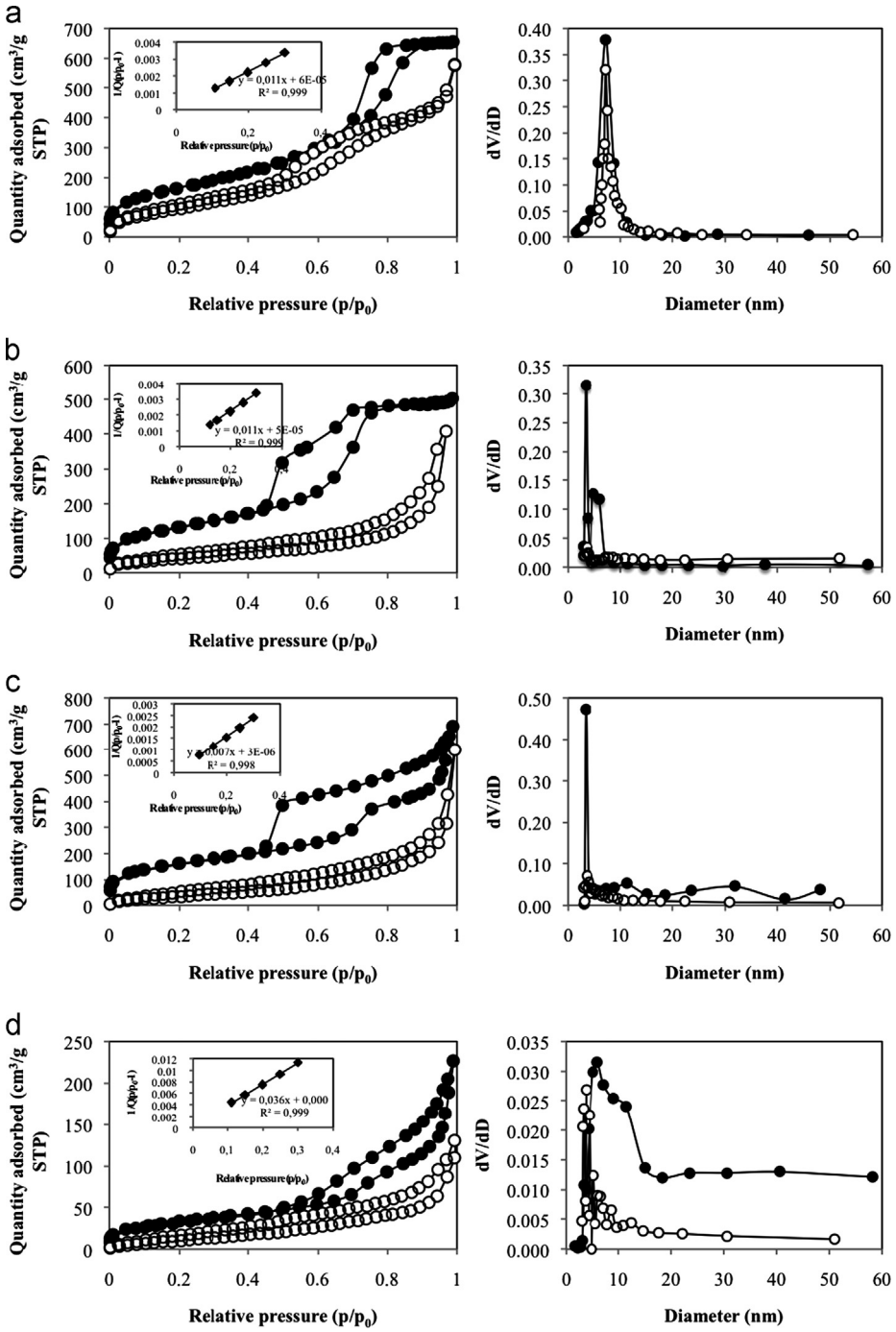

Fig. 4. Evolution of nitrogen adsorption–desorption isotherms for materials before IBU adsorption (black points) and after IBU adsorption (white points) and BJH pore sized distributions for (a) material obtained without oil fraction, (b) material obtained from 0.20 of dispersed phase, (c) material obtained from 0.50 of dispersed phase and (d) material obtained from 0.75 of dispersed phase. *T*-plot for materials before IBU adsorption is shown.

T-plot analysis is shown for the obtained materials. In all cases the *Y*-intercept was zero, which would indicate a lack of microporosity, so all the specific surfaces of the materials were due to mesoporosity and macroporosity.

When the dispersed phase fraction was increased from 0.00 to 0.75, a decrease in the specific area from 600 to 154 m^2/g (Chart 1) was observed. This has been shown by other authors [43] and could be explained by the fact that when the quantity of oil in the emulsion is increased, the interphase oil–water also increases and the surfactant preferably locates in this interphase, thus stabilizing the emulsion. This causes a reduction of free surfactant in the water. Therefore, the higher the dispersed phase fraction used, the less surfactant is available to form the mesostructure in the continuous phase and the lower the density of ordered mesopores, deriving into a smaller specific area, since the S_{BET} only considers the contribution of the meso-sized pores. Another possible explanation for this is that silica tends to polymerize and accumulate in the interphases, which do not present mesoporous structures. Therefore, the higher the dispersed phase fraction used, the less structure there is and, consequently, the less specific surface there is. Both of these mechanisms could contribute to decreasing the specific surface with dispersed phase.

Chart 1 shows how the average diameter of the mesopores remains approximately constant up to a dispersed phase fraction

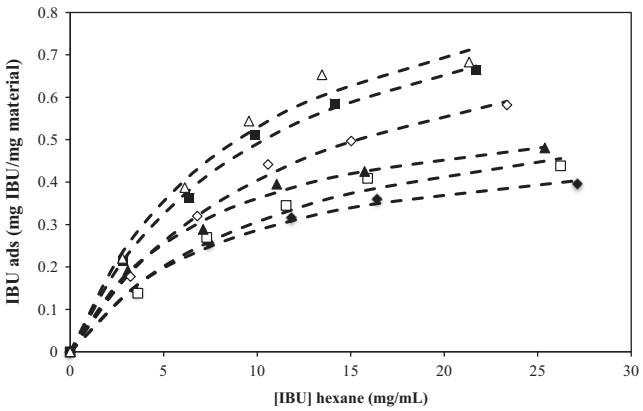

Fig. 5. Adsorption isotherms of Ibuprofen release profiles for the materials obtained from samples P84_meso (black diamonds), P84_20% (white squares), P84_50% (black triangles), P84_75% (white diamonds), P84_75% functionalized by grafting (black squares) and P84_75% functionalized by co-condensation method (white triangles).

Chart 2
Fitting parameters obtained from Langmuir equation.

Experiment	Γ_{max} (mg IBU/mg mat)	k	R^2
P84_meso	0.53	0.12	0.991
P84_20%	0.65	0.09	0.962
P84_50%	0.62	0.14	0.994
P84_75%	0.90	0.08	0.989
P84_75%_grafting	0.99	0.10	0.991
P84_75%_co-condensación	1.02	0.11	0.969

of 0.50, and increases from 4.1 to 8.5 nm when the dispersed phase fraction is increased from 0.50 to 0.75. The addition of oil acts as a swelling agent, as previously reported [45,46], and this could increase the size of the mesopores obtained. Decane reduces the hydration of the hydrophobic poly(propylene oxide) (PPO) chains. It is also located in the micelle core and acts as a swelling agent and can therefore be used to control pore size.

3.2. Ibuprofen adsorption isotherm.

The adsorption of IBU from hexane was studied by determining the adsorption isotherms for the materials prepared with different dispersed phase contents, described in Chart 1, and for the functionalized materials. Adsorption equilibrium curves are represented in Fig. 5.

The Langmuir adsorption equation could be expressed as:

$$\Gamma = \Gamma_{max}\frac{k \times c}{(1+k \times c)} \quad (1)$$

where k, represents the Langmuir constant, c the equilibrium concentration of IBU in hexane solution, and Γ_{max} the maximum amount of IBU adsorbed per weight of material. k and Γ_{max} were determined by Lineweaver–Burk linearization.

The first step of the adsorption process is the migration of the IBU molecules from a bulk solution to the surface. The second was adsorption on the material surface and diffusion into the interior pores of the silica materials. The increase in IBU concentration would be in favour of IBU migration to the surface and diffusion into the interior pores of the materials until equilibrium is reached.

Chart 2 shows the Langmuir isotherm fitting parameters obtained from the experimental data. The maximum IBU weight adsorbed for weight of mesoporous material increases when the macropore presence increases and improves with functionalization. It can be observed two R values, for P84_20% and P84_75%_co.condensation, quite low. This is due to the two experimental data from theoretical isotherm. Concentrations are quite low, so a small deviation results into a low fitting parameter. For the other samples the fitting parameters are good.

Fig. 5 shows that mesoporous materials have a lower adsorption capacity than materials with macropores in their structure, in spite of the higher S_{BET}. It could be concluded that, as increasing the macropores present in the material increase the access of IBU to all specific areas, particularly the internal porous area, is enhanced. Although the S_{BET} of the meso–macroporous materials are lower than the S_{BET} of the mesoporous material - in the case of the material P84_75% the specific area is four times lower—the accessible area is bigger when macropores are present as they allow the IBU molecules to diffuse towards the surface of internal mesopores, while the IBU adsorbed on mesoporous materials is probably located in the external part of the mesochannels, which they rapidly obturate and, therefore, the rest of the remaining mesochannels are not used.

The material P84_75% was functionalized in order to increase IBU adsorption on the silica as a result of the amino groups that provide a stronger interaction with the OH group of the ibuprofen. Two mechanism were used, i.e.the grafting process and co-condensation. In order to verify the amino groups present in the material, the materials were characterized by FT-IR (Fig. 6).

The asymmetric vibrations of the Si–O–Si bonds appear around 1070 cm^{-1}, as can be observed in the spectra of Fig. 6a, which corresponds to the meso–macroporous material with a dispersed phase of 75%. This band remains constant in the other materials: in the case of the material functionalized using the grafting process with APTES, the sample presents a band at3200 cm^{-1}, corresponding to the C–H bond, and a smaller band at 1540 cm^{-1} due the vibrations of the N–H bond. The C–H and N–H bonds correspond to the aminopropyl groups grafted in the surface of the silica material [34,47,48].

The FT-IR spectra for the material functionalized with the co-condensation process (Fig. 6c) shows more intense bands corresponding to the C–H and N–H bond, indicating the presence of more amino groups using this technique, which produces more homogeneity in the amine distribution on the material surface.

The FT-IR spectra for the samples with IBU adsorbed are shown in Fig. 6d, in the case of the material functionalized by grafting, and Fig. 6e, in the case of that functionalized using the co-condensation method. In both spectra, the bands at 3200 and 1500 cm^{-1}, corresponding to the C–H and phenyl group, respectively can be conserved. The observed band at 1710 cm^{-1} in the P84_75%_co-condesation_IBU is due to the COOH group of the ibuprofen molecule while the peaks at 1555 cm^{-1} in the spectra are indicative of the formation of the $COO^{-}NH_3^{+}$ bond [48]. Fig. 6f shows FT-IR spectra for ibuprofen molecule. For low wavenumber region many peaks are observed as other authors reported [49,50]. This is also appreciated in the samples loaded with ibuprofen for P84_75% functionalized by grafting method and more obviously with functionalized by co-condensation method due. These peaks are due to a high level of ibuprofen, so FT-IR spectra is more similar to the ibuprofen spectra than the material without drug loading.

3.3. Ibuprofen release experiments.

The amount of drug released from a film or thin disk is proportional to the square root of the time (Higuchi model) [25], and the release speed decreases gradually. The kinetics of the release process is governed by the physical properties, particularly by its molecular weight and the solubility of the polymeric matrix and the quantity of drug incorporated. The diffusion speed

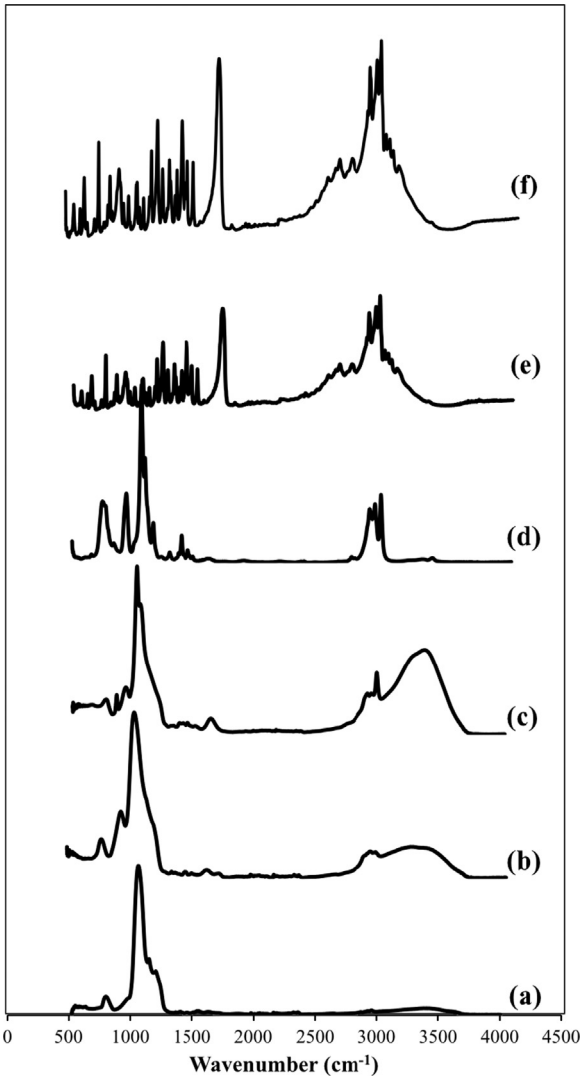

Fig. 6. FT-IR spectra for the (a) P84_75%, (b) P84_75%_grafting, (c) P84_75%_co-condensation, (d) P84_75%_grafting_IBU, (e) P84_75%_co-condensation_IBU and (f) IBU.

depends on the specific area and the matrix density, as well as the diffussion coefficient of the drug. If there is enough drug to maintain the internal concentration at higher levels than the concentration in the external media, the diffusion speed of the drug through the matrix is constant.

In vitro controlled release was carried out in order to check the properties and behaviour of the materials. Fig. 7 the percentage of IBU released as a function of time.

The first release is attributed to the so-called burst effect as Gallagher and Corrigan postulated in their model [51]. This effect is due to the fact that ibuprofen molecules are physically adsorbed on the outer surface of the material and these molecules, which are more accessible, are rapidly released, as other authors have observed [52,53]. The second stage corresponds to the slow diffusion of ibuprofen molecules from the mesochannels of the material to the media, along the macroporous channels.

It is clear that all the materials present a first stage called the burst stage, where a significant amount of IBU is released in less than 10 h, as can be observed by zooming in on Fig. 7. This fast release is due to the desorption of the IBU molecules adsorbed in the external part of the mesochannels. Therefore, when the release process starts, these molecules are the first to migrate to the media. For the mesoporous material, the burst effect reaches 96% of the ibuprofen release; for the material with a dispersed phase of 20% this value was around 83%; for the material with a dispersed phase of 50% the release of IBU in the burst stage was 79%; and for the material with a dispersed phase of 75%, this value dropped to 63% of the IBU. According to these results, we can assume that the macropore presence in the material facilitates the release of the drug and minimizes the burst effect.

This fact may seem strange, because the macropore channels should ease the diffusion from the mesostructure to the media. However, it has been shown in previous sections that macropores favour the access of IBU molecules to all available mesopores, including the internal pores, since the adsorption capacity of meso–macroporous materials is higher than that of mesoporous materials, in spite of their smaller S_{BET}. Moreover, the mesostructure for meso–macroporous materials presented bigger pore sizes than the mesopores obtained in the mesoporous materials (Chart 1), which again favours once more a deeper penetration of IBU along the mesochannels. The relese of ibuprofen from the mesoporous material was faster, because the IBU molecules were located on the external surface or in the outer surface of the mesochannels, since they could not penetrate much due to the fact that some of the IBU molecules adsorbed obstructed the mesochannels. On the other hand, during the release experiments, the bath containing the SBF solution was under gently agitated to ensure that there were no privileged diffusion paths. Due to this gentle agitation, the IBU molecules of the mesoporous material that were not located in the deeper material structure had an enhanced rate of transfer. In the case of the meso–macroporous materials, the IBU molecules should have moved through the macropores channels, where there was no agitation and which were acting as an additional diffusion barrier that the IBU molecules located in external mesopores would not encounter.

Fengyu Qu et al. [49] observed that meso–macroporous material obtained from natural substances presented an IBU release of 60% at 50 h compared to the 100% release for mesoporous material. In our case, at 50 h the material with a dispersed phase of 75% presented an IBU delivery rate of 60%, while for mesoporous material, it reached 96%. The meso–macroporous material containing a disperse phase of 75% reached the total IBU release at 120 h.

The functionalized material is shown to present a higher adsorption capacity and a slower release of IBU in compared to the material without amino groups. In the case of the grafting method, the reduction in release velocity is not significant, but in the case of the co-condensation sample, a significant decrease in the release of IBU with time can be observed, due to the improvement and more homogeneous functionalization of the material. In co-condensation method the amino groups were introduced during the formation of the material, so the internal walls of the macropores and mesopores were filled with more amino groups than the walls of the material functionalized by post-grafting method. Post-grafting method introduces more amino groups on the external surface because the material was previously formed. For this reason, the adsorption properties are quite similar in both techniques but the release was slower in the case of co-condensation, due to the amino groups and ibuprofen are linked in the internal surface. The burst stage is reduced from 60% for the P84_75% to 45% for the P84_75%_co-condensation sample.

4. Conclusions

In this paper hierarchically meso–macroporous materials were obtained using an ordered mesostructure. Materials were studied as drug delivery systems, and ibuprofen was chosen as a model drug. The adsorption capacities and release behaviours of the

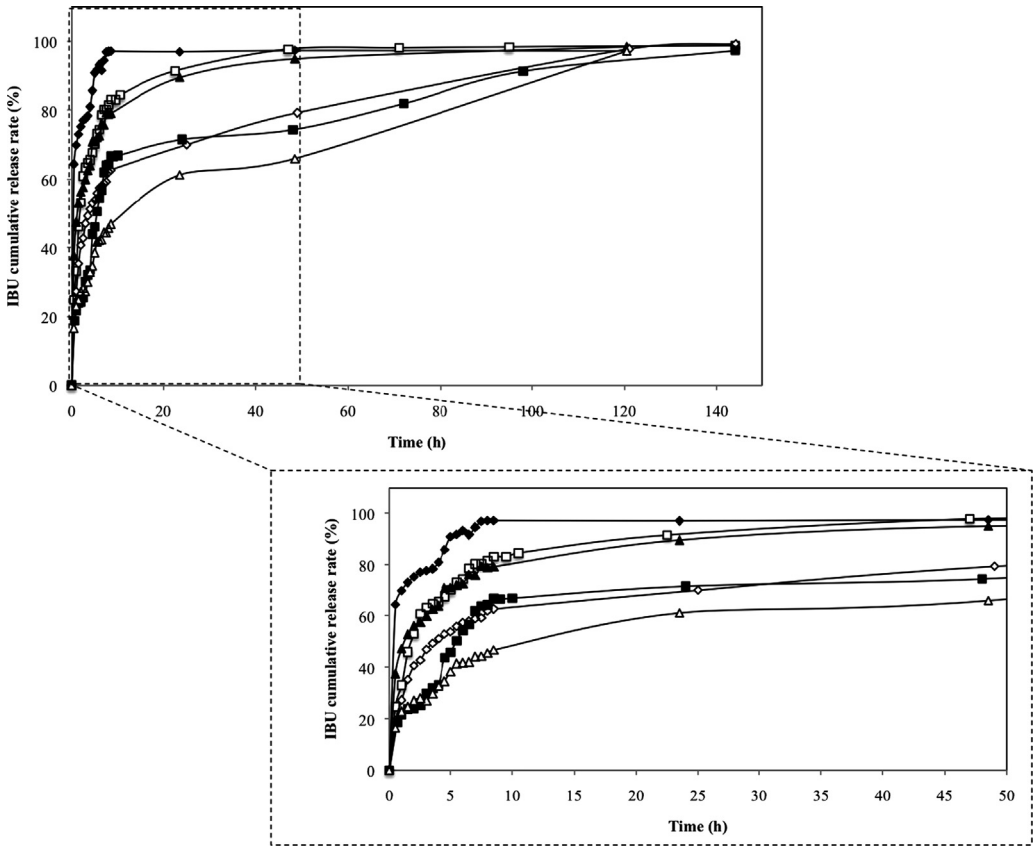

Fig. 7. Ibuprofen release profiles for the materials obtained from samples P84_meso (black diamonds), P84_20% (white squares), P84_50% (black triangles), P84_75% (white diamonds), P84_75% functionalized by grafting (black squares) and P84_75% functionalized by co-condensation method (white triangles).

model drug were highly dependent on the structure of the materials. The IBU amount adsorbed was mainly a function of the quantity of macropores present in the material due the fact that macropores allowed the drug molecules to penetrate deeper pores, thus covering a higher surface area of the material. For the release process, two-steps were observed; these consisted of an initial fast release, called the burst effect, which is related to the liberation of the IBU adsorbed in pores near the surface of the material, and a subsequent slower release, relating to the desorption of drug molecules adsorbed at pores located further inside the surface of the material, which should diffuse along the macropore channels. While the presence of macropores is increased the burst effect is minimized and the delivery is more sustained over time. The materials with more macropores present a slower release rate, since the IBU molecules are located over all the material's surface and not only near the surface of the material. During the release experiments, first the molecules on the external surface were released first, followed by the molecules in the deeper structure. Therefore, we can conclude that for meso–maroporous materials, the drug molecules must overcome two diffusion barriers, one corresponding to the macropore channel and the other corresponding to the diffusion from the material to the fluid. The co-condensation method to functionalize materials presents a higher capacity to adsorb IBU and a slower release rate than the material functionalized using the grafting method due to a more homogeneous functionalization.

Acknowledgments

This study would not have been possible without the financial support from the Spanish Ministry of Science and Innovation (MICINN) within the framework of the project CTQ2011-29336-C03-02. Thanks to SAXS measurements done by the Consejo Superior de Investigaciones Científicas (CSIC). To Mr. Jonathan Miras, Mrs Maria Martínez for their advice with SAXS results.

References

[1] W.J. Koros, Y.H. Ma, T. Shimidzu, Terminology for membranes and membrane processes, J. Membr. Sci. 120 (1996) 149.
[2] C.T. Kresge, M.E. Leonowicz, W.J. Roth, J.S. Beck, Ordered mesoporous molecular sieves synthetized by a liquid-crystal template mechanism, Nature 359 (1992) 710.
[3] J.S. Beck, J.C. Vartuli, W.J. Roth, M.E. Leonowicz, C.T. Kresge, K.D Schmitt, C.T. W Chu, D.H. Olson, E.W. Sheppard, S.B. McCulle, J.B. Higgins, J.L. Schlender, A new family of mesoporous molecular sieves prepared with liquid crystal templates, J. Am. Chem. Soc. 114 (1992) 10834–10843.
[4] Y. Wan, D. Zhao, On the controllable soft templating approach to mesoporous silicates, Chem. Rev. 107 (2007) 2821.
[5] Shao-Ting Wang, Ming-Luan Chen, Yu-Qi Feng, A meso–macroporous borosilicate monoliths prepared by a sol–gel method, Microporous Mesoporous Mater. 151 (2012) 250–252.
[6] Abbas Khaleel, Shamsa Al-Mansouri, Meso–macroporous g-alumina by tenplate-free sol–gel synthesis: the effect of the solvent and acid catalyst on the microstructure and textural properties, Colloids Surf., A 369 (2010) 272–280.
[7] Arnaud Lemaire, Bao-Lian Su, Highly spongy hierarchical structured meso–macroporous aluminosilicates with high tetrahedral aluminum content and 3D interconnectivity from a single-source molecular precursor (sec-BuO)2-Al–O–Si(OEt)3: effect of silicon co-reactant, Microporous Mesoporous Mater. 142 (2011) 70–81.
[8] Z.Y. Yuan, B.L. Su, Insights into hierachically meso–macroporous structured materials, J. Mater. Chem. 16 (2006) 663.
[9] P. Diddams, Inorganic Supports and Catalysts, Ellis Horwood, New York, 1992.
[10] J.Y. Ying, C.P. Mehnert, M.S. Wong, Synthesis and applications of supramolecular-templated mesoporous materials, Angew. Chem. Int. Ed. Engl. 38 (1999) 56–77.
[11] Z.Y. Yuan, T.-Z. Ren, A. Vantomme, B.-L. Su, Facile and generalized preparation of hierarchically mesoporous–macroporous binary metal oxide materials, Chem. Mater. 16 (2004) 5096–5106.

[12] C. Groen, W. Zhu, S. Brouwer, S.J. Huynink, F. Kapteijn, J.A. Moulijn, J. Pérez-Ramírez, Direct demonstration of enhanced diffusion in mesoporous ZSM-5 zeolite obtained via controlled desilication, J. Am. Chem. Soc. 129 (2007) 355–360.
[13] A. Imhof, D.J. Pine, Ordered macroporous materials by emulsion templating, Nature 389 (30) (1997) 948.
[14] C. Solans, J. Esquena, N. Azemar, Highly concentrated (gel) emulsions, versatile reaction media, Curr. Opin. Colloid Interface Sci. 8 (2003) 156–163.
[15] J.M. Kim, G.D. Stucky, Synthesis of highly ordered mesoporous silica materials using sodium silicate and amphiphilic block copolymers, Chem. Commun. (2000) 1159–1160.
[16] M. Vallet-Regi, A. Ramila, R.P. del Real, J. Perez-Pariente, A new property of MCM-41: drug delivery system, Chem. Mater. 13 (2001) 308–311.
[17] J. Anderson, J. Rosenholm, S. Areva, M. Linden, Influences of material characteristics on ibuprofen drug loading and release profiles from ordered micro- and mesoporous silica matrices, Chem. Mater. 16 (2004) 4160–4167.
[18] E. Ruiz-Hernandez, A. Lopez-Noriega, D. Arcos, I. Izquierdo-Barba, O. Terasaki, M. Vallet-Regi, Aerosol—assisted synthesis of magnetic mesoporous silica spheres for drug targeting, Chem. Mater. 19 (2007) 3455–3463.
[19] P. Horcajada, A. Ramila, J. Perez-Pariente, M. Vallet-Regi, Influence of pore size of MCM-41 matrices on drug delivery rate, Microporous Mesoporous Mater. 68 (2004) 105–109.
[20] T. Heikkila, J. Salonen, J. Tuura, M.S. Hamdy, G. Mul, N. Kumar, T. Salmi, D. Y. Murzin, L. Laitinen, A.M. Kaukonen, J. Hirvonen, V.P. Lehto, Mesoporous silica material TUD-1 as a drug delivery system, Int. J. Pharm. 331 (2007) 133–138.
[21] B. Munoz, A. Ramila, J. Perez-Pariente, I. Diaz, M. Vallet-Regi, MCM-41 organic modification as drug delivery rate regulator, Chem. Mater. 15 (2003) 500–503.
[22] Y.F. Zhu, J.L. Shi, Y.S. Li, H.R. Chen, W.H. Shen, X.P. Dong, Hollow mesoporous spheres with cubic pore network as a potential carrier for drug storage and its in vitro release kinetics, J. Mater. Res. 20 (1) (2005) 54–61.
[23] S.W. Song, K. Hidajat, Functionalized SBA-15 materials as carriers for controlled drug delivery: influence of surface properties on matrix-drug interactions, Langmuir 21 (2005) 9568–9575.
[24] S.S. Huang, Y. Fan, Z.Y. Cheng, D.Y. Kong, P.P. Yang, Z.W. Quan, C.M. Zhang, J. Lin, Magnetic mesoporous silica spheres for drug targeting and controlled release, J. Phys. Chem. C 113 (2009) 1775–1784.
[25] Xiufang Wang, Ping LiuYong Tian, Ordered mesoporous carbons for ibuprofen drug loading and release behavior, Microporous Mesoporous Mater. 142 (2011) 334–340.
[26] Shaobin Wang, Ordered mesoporous materials for drug delivery, Microporous Mesoporous Mater. 117 (2009) 1–9.
[27] B. González, M. Colilla, M. Vallet-Regi, Time-delayed release of bioencapsulates: a novel controlled delivery concept for bone implant technologies, Chem. Mater. 20 (2008) 4826–4834.
[28] Q. Tang, Y. Xu, D. Wu, Y. Sun, A study of carboxylic-modified mesoporous silica in controlled delivery for drug famotidine, J. Solid State Chem. 179 (2006) 1513–1520.
[29] K.K. Sharma, T. Asefa, Efficient bifunvtional nanocatalysts by simple postgrafting of spatially isolated catalutic groups on mesoporous materials, Angew. Chem. Int. Ed. 46 (2007) 2879–2882.
[30] I.I. Slowing, B.G. Trewyn, S. Giri, V.Y. Lin, Mesoporous silica nanoparticles for drug delivery and biosensing applications, Adv. Funct. Mater. 17 (2007) 1225–1236.
[31] H. Vallhov, S. Gabrielsson, M. Stromme, A. Scheynius, A.E. Garcia-Bennett, Mesoporous silica particles induce size dependent effects on human dendritic cells, Nano Lett. 7 (2007) 3576.
[32] J.A. Melero, R. van Grieken, G. Morales, Advances in the synthesis and catalytic applications of organosulfonic functionalized mesostructured materials, Chem. Rev. 106 (2006) 3790–3812.
[33] S. Huh, J.W. Wiench, J.C. Yoo, M. Pruski, V.Y. Lin, Organic functionalization and morphology control of mesoporous silicas via a co-condensation synthesis method, Chem. Mater. 15 (2003) 4247–4256.
[34] A. Szegedi, M. Popova, I. Goshev, J. Mihaly, Effect of amine functionalization of spherical MCM-41 and SBA-15 on controlled drug release, J. Solid State Chem. 184 (2011) 1201–1207.
[35] Gang Wang, Amy N. Otuonye, Elizabeth A. Blair, Kelley Denton, Zhimin Tao, Tewodros Asefa, Functionalized mesoporous materials for adsorption and release of different drug molecules: a comparative study, J. Solid State Chem. 182 (2009) 1649–1660.
[36] T. Kokubo, H. Kushitani, S. Sakka, T. Kitsugi, T. Yamamuro, Solutions able to reproduce in vivo surface-structure changes in bioactive glass–ceramic A–W, J. Biomed. Mater. Res. 24 (1990) 721–734.
[37] S.B. Cho, K. Nakanishi, T. Kokubo, N. Soga, C. Ohtsuki, T. Nakamura, T. Kitsugi, T. Yamamuro, Dependence of apatite formation on silica gel on its structure: effect of heat treatment, J. Am. Ceram. Soc. 78 (1995) 1769–1774.
[38] D.Y. Zhao, J.L. Feng, Q.S. Huo, N. Melosh, G.H. Fredrickson, B.F. Chmelka, G.D. Stucky, Triblock copolymer syntheses of mesoporous silica with periodic 50 to 300 angstrom pores, Science 279 (1998) 548–552.
[39] C.Z. Yu, J. Fan, B.Z. Tian, D.Y. Zhao, G.D. Stucky, High-yield synthesis of periodic mesoporous silica rods and their replication to mesoporous carbon rods, Adv. Mater. 14 (2002) 1742.
[40] H.F. Yang, Q.H. Shi, B.Z. Tian, S.H. Xie, F.Q. Zhang, Y. Yan, B. Tu, D.Y. Zhao, A fast way for preparing crack-free mesostructured silica monolith, Chem. Mater. 15 (2003) 536–541.
[41] D.Y. Zhao, P.D. Yang, B.F. Chmelka, G.D. Stucky, Multiphase assembly of mesoporous–macroporous membranes, Chem. Mater. 11 (1999) 1174.
[42] N. Du, M.J. Stébé, R. Bleta, J.L. Blin, Preparation and characterization of porous silica templated by a nonionic fluorinated Systems, Colloids Surf., A 357 (2010) 116–127.
[43] J.L. Blin, R. Bleta, J. Ghanbaja, M.J. Stébé, Fluorinated emulsions: templates for the direct preparation of macropores–mesoporous silica with a highly ordered array of large mesoporous, Microporous Mesoporous Mater. 94 (2006) 74–80.
[44] S. Brunauer, L.S. Deming, W.S. Deming, E. Teller, On a theory of the van der Waals adsorption of gases, J. Am. Chem. Soc. 62 (1940) 1723–1732.
[45] E.M. Johansson, Mohamed A. Ballem, José M. Córdoba, Magnus Odén, Rapid synthesis of SBA-15 rods with variable lengths, widths, and tunable large pores, Langmuir 27 (2011) 4994–4999.
[46] E.M. Johansson, J.M Córdoba, M. Odén, The effects on pore size and particle morphology of heptane additions to the synthesis of mesoporous silica SBA-15, Microporous Mesoporous Mater. 133 (2010) 66–74.
[47] Sh.Xing Wang, Y. Zhou, W. Guan, B. Ding, Preparation and characterization of stimuli-responsive magnetic, nanoparticles, Nanoscale Res. Lett. 3 (2008) 289–294.
[48] Y.J. Yang, X. Tao, Q. Hou, J.-F. Chen, Fluorescent mesoporous silica nanotubes incorporating CdS quantum dots for controlled release of ibuprofen, Acta Biomater. 5 (2009) 3488–3496.
[49] Fengyu Qu, Huiming Lin, Xiang Wu, Xiaofeng Li, Shilun Qiu, Guangshan Zhu, Bio-templated synthesis of highly ordered macro-mesoporous silica material for sustained drug delivery, Solid State Sci. 12 (2010) 851–856.
[50] Fengyu Qu, Guangshan Zhu, Huiming Lin, Weiwei Zhang, Jinyu Sun, Shougui Li, Shilun Qiu, A controlled release of ibuprofen by systematically tailoring the morphology og mesoporous silica material, J. Solid State Chem. 179 (2006) 2027–2035.
[51] K.M. Gallagher, O.I. Corrigan, Mechanistic aspects of the release of levamisole hydrochloride from biodegradable polymers, J. Controlled Release 69 (2000) 261–272.
[52] M. Vallet-Regí, J.C. Doadrio, A.L. Doadrio, I. Izquierdo-Barba, J. Pe rez-Pariente, Hexagonal ordered mesoporous material as a matrix for the controlled release of amoxicillin, Solid State Ionics 172 (2004) 435–439.
[53] C. Charnay, S. Bégu, C. Tourné-Péteilh, L. Nicole, D.A. Lerner, J.M. Devoisselle, Inclusion of ibuprofen in mesoporous templated silica: drug loading and release property, Eur. J. Pharm. Biopharm. 57 (2004) 533–540.